

The effect of torsion on the motion of a helical vortex filament

By RENZO L. RICCA

Department of Mathematics, University College London,
Gower Street, London WC1E 6BT, UK

(Received 27 April 1993 and in revised form 24 February 1994)

In this paper we analyse in detail, and for the first time, the rôle of torsion in the dynamics of twisted vortex filaments. We demonstrate that torsion may influence considerably the motion of helical vortex filaments in an incompressible perfect fluid. The binormal component of the induced velocity, asymptotically responsible for the displacement of the vortex filament in the fluid, is closely analysed. The study is performed by applying the prescription of Moore & Saffman (1972) to helices of any pitch and a new asymptotic integral formula is derived. We give a rigorous proof that the Kelvin régime and its limit behaviour are obtained as a limit form of that integral asymptotic formula. The results are compared with new calculations based on the re-elaboration of Hardin's (1982) approach and with results obtained by Levy & Forsdyke (1928) and Widnall (1972) for helices of small pitch, here also re-elaborated for the purpose.

1. Introduction

Many computational simulations show (Siggia 1981; Kerr 1985; Vincent & Meneguzzi 1991; Kida 1993) that highly twisted vortex tubes constitute a fundamental structural element in the evolution of turbulent flows. Experimental evidence (see, for example, Hopfinger, Browand & Gagne 1982; Leibovich & Ma 1983; Maxworthy, Hopfinger & Redekopp 1985) and numerical results (see, for example, She, Jackson & Orszag 1990; Lesieur 1991; Boratav, Pelz & Zabusky 1992) show clearly that torsion of vortex tubes plays an important rôle in three-dimensional vortex evolution. Torsion is the essential geometric property of structures that are truly three-dimensional and is certainly important in regions of high helicity and high twisting of vorticity lines. In particular, it has been observed (Hopfinger *et al.* 1982; Leibovich & Ma 1983) that torsion may have a significant effect on the dynamics of twisted vortex filaments. In this paper we demonstrate, for the first time, that indeed torsion may influence considerably the motion of helical vortex filaments.

The study of the motion of helical and generally twisted vortex filaments in an incompressible perfect fluid has a long history. A first study of the dynamics of slightly twisted vortex filaments was carried out by Lord Kelvin (1880) for helical vortex filaments of very large pitch (i.e. very large wavelength). Some time later, Levy & Forsdyke (1928) considered the case of helices of small pitch. A great deal of difficulty in the analysis is due to the treatment of the logarithmic singularity present in the Biot-Savart integral. To see this, let us denote by $\mathbf{u} = \mathbf{u}(X)$ the velocity induced by a helical vortex filament \mathcal{H} at a neighbouring point X and let $X^* = X^*(s)$ be the helical vortex filament axis (s being arclength). For simplicity, let us assume that the

vorticity $\omega(X^*) = \omega_0 \mathbf{t}$, with $\omega_0 = \text{constant}$ and \mathbf{t} the tangent to X^* , be uniformly distributed across a circular cross-section of area $\pi\sigma^2$ and vortex core circulation $\kappa = \omega_0\pi\sigma^2$. The induced velocity is given by the Biot-Savart law

$$\mathbf{u}(X) = \frac{\kappa}{4\pi} \int_{\mathcal{V}} \frac{\mathbf{t}(X^*) \times (X - X^*)}{|X - X^*|^3} ds. \quad (1.1)$$

A simple and direct calculation of (1.1) for a thin vortex filament was given by Batchelor (1967, p. 510). Batchelor's formula gives the asymptotic velocity

$$\mathbf{u}^{(a)} = \frac{\kappa}{2\pi\sigma} \mathbf{q} + \frac{\kappa}{4\pi R} \ln \frac{L}{\sigma} \mathbf{b} + \mathbf{Q}_f, \quad (1.2)$$

where σ denotes distance from the filament axis in a normal plane, \mathbf{q} is a rotational unit vector about the filament axis, R is the local radius of curvature, L is a length parameter that takes into account the short-range inductive effects due to neighbouring parts of the vortex filament ($\sigma < L \ll R$), \mathbf{b} is the binormal vector to the filament axis and \mathbf{Q}_f denotes the finite-term contribution due to the induction of distant parts of the vortex filament. L and \mathbf{Q}_f are left undetermined in Batchelor's formula. Evidently, the first term in the right-hand side of (1.2) yields a rotational motion about the vortex filament axis, with no contribution to the relative displacement of the vortex in the fluid, while the second term yields a displacement of the vortex filament along its local binormal direction, and depends, in first approximation, on the circulation and the geometric properties of the vortex filament centreline. The binormal component of the drift velocity $\mathbf{v}^{(a)} = \mathbf{u}^{(a)} - [\kappa/(2\pi\sigma)]\mathbf{q}$ can be written in dimensionless form (i.e. dividing by the reference velocity $\kappa/4\pi R$), and is given by

$$\hat{\mathbf{v}}_b^{(a)} = \ln \frac{L}{\sigma} + \hat{\mathbf{Q}}_f \cdot \mathbf{b} = \ln \frac{R}{\sigma} + C, \quad (1.3)$$

where C , a function only of the geometry, denotes the remainder term.

From a historical point of view it is interesting to note that equation (1.2) was actually derived by Levi-Civita (1932, p. 26, equation 6) as a particular case of a slightly more general equation found in his study on vortex filaments.

The logarithmic singularity that arises in (1.3) as $\sigma \rightarrow 0$ is trivially avoided if the Biot-Savart integral is evaluated at some finite distance from the vortex filament axis, with an approximate estimate of the induced velocity. An alternative solution is offered by the so-called 'cut-off' technique (Crow 1970). Based on the fact that the velocity of a vortex ring is completely known (Fraenkel 1970; Saffman 1970), the 'cut-off' method consists of 'de-singularizing' the Biot-Savart integral by removing a small arc interval which contains the singularity, and replacing its contribution by the corresponding (known) contribution of the osculating vortex ring. The stability of helical vortex filaments of small pitch was investigated by Widnall (1972) using the 'cut-off' approximation and numerical integration.

Following the idea of balancing the fluid dynamical forces that act on a vortex filament (Widnall & Bliss 1971; Widnall, Bliss & Zalay 1971), Moore & Saffman (1972) proposed an analytic prescription for evaluating Biot-Savart. It is based on the idea of de-singularizing the Biot-Savart integral in an analytical way, by subtracting and adding the contribution given by a (virtual) osculating circular vortex filament with the same local vortex core properties. A comparison between the velocity calculated by the cut-off approximation and that calculated using this latter prescription showed (cf. Moore & Saffman 1972, p. 417) that the two methods are almost equivalent when axial velocities within the vortex tube are not present. The Moore & Saffman

prescription, however, has not been used so far, and its application is presented here for the first time.

An explicit analytic solution for the velocity field induced by a helical vortex filament, evaluated at distant points in the interior and exterior of the circular cylinder on which the helix is inscribed, is due to Hardin (1982). Hardin's approach is based on a suitable transform of the Biot-Savart integral and can capture higher-order effects; however, he made no effort to give the velocity an asymptotic expression and only recently (Ricca 1992, 1993) has a full numerical investigation of the asymptotic behaviour of this velocity field been carried out. Several other equations of motion able to capture a variety of physical aspects (for example in the presence of axial and swirl velocities, vortex core perturbations, viscous effects) have been presented in the literature (Callegari & Ting 1978; Adebisi 1981; Fukumoto & Miyazaki 1991; Lundgren & Ashurst 1989; Marshall 1991; Klein & Majda 1991), but the methods discussed above remain fundamental.

In this paper we analyse in detail, and for the first time, the rôle of torsion in the dynamics of twisted vortex filaments. We demonstrate that torsion may influence considerably the motion of helical vortex filaments in an incompressible perfect fluid. The work is organized as follows. In §2 we recall some basic geometric relations. In particular, we consider a one-parameter family of helices of equal curvature (which is kept constant) and different torsion. In §3 we apply the prescription of Moore & Saffman to study helices of any pitch. The asymptotic velocity of the helical vortex filament is decomposed into intrinsic components and a new integral asymptotic formula for the binormal component of the induced velocity is found as a function of the geometry alone. We present calculations based on this new formula and, in §3.1, we give a rigorous proof that Kelvin's régime is obtained as a limit form of this integral formula for helices of large pitch.

A full comparative analysis of these new results is carried out in §4. New calculations based on the re-elaboration of Hardin's (1982) approach are presented in §4.1, together with a brief discussion of the two limit cases represented by the rectilinear vortex filament (when the pitch tends to infinity) and the circular cylindrical vortex sheet (when the pitch tends to zero). Results obtained by Levy & Forsdyke (1928) and Widnall (1972) for helices of small pitch are then re-elaborated and presented for comparison (§4.2). The agreement between different treatments is satisfactory and proves a clear influence of torsion on the vortex filament motion. The conclusions are summarized in §5.

2. Geometric relations for a helical vortex filament

Let us consider an infinite right-handed helical vortex filament embedded in an incompressible perfect fluid at rest at infinity. For the sake of simplicity the study is carried out by assuming that the tube-like vortex has a core of circular cross-section, whose radius is negligible compared with the local radius of curvature, and that the vorticity is (instantaneously) uniformly distributed across the circular cross-section and directed everywhere parallel to the tangent to the vortex filament centreline \mathcal{H} . This centreline is represented by the helix $X^* = (x, y, z)$

$$x = r_0 \cos \alpha, \quad y = r_0 \sin \alpha, \quad z = p\alpha, \quad (2.1)$$

where r_0 is the radius of the circular cylinder on which the helix is inscribed, α is the polar angle, and p is the (reduced) pitch of the helix (that is the distance between

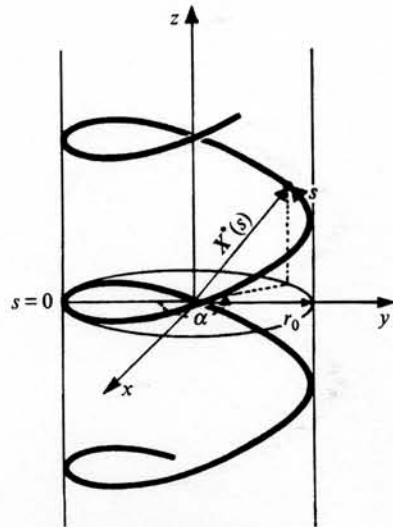


FIGURE 1. Geometry of the helical vortex filament.

two consecutive coils measured in the direction parallel to the z -axis, divided by 2π) (figure 1). In cylindrical polar coordinates \mathcal{H} is labelled by $X^* = (r_0, \alpha, z)$.

The arclength s of \mathcal{H} is given by

$$s = \alpha (r_0^2 + p^2)^{\frac{1}{2}} \quad (s = 0 \text{ for } \alpha = 0), \quad (2.2)$$

so that, after substitution of (2.2) into (2.1), we can write the curve in intrinsic form $X^* = X^*(s)$ and determine the intrinsic reference frame (the Frenet frame) $(\mathbf{t}, \mathbf{n}, \mathbf{b})$ (Willmore 1959). By definition of unit tangent we have

$$\mathbf{t} = X' = \frac{r_0}{(r_0^2 + p^2)^{\frac{1}{2}}} \left[-\sin \left(\frac{s}{(r_0^2 + p^2)^{\frac{1}{2}}} \right), \cos \left(\frac{s}{(r_0^2 + p^2)^{\frac{1}{2}}} \right), \frac{p}{r_0} \right], \quad (2.3)$$

where the prime denotes differentiation with respect to arclength. By further differentiation, we have the unit normal

$$\mathbf{n} = \frac{X''}{|X''|} = \left[-\cos \left(\frac{s}{(r_0^2 + p^2)^{\frac{1}{2}}} \right), -\sin \left(\frac{s}{(r_0^2 + p^2)^{\frac{1}{2}}} \right), 0 \right], \quad (2.4)$$

and binormal

$$\mathbf{b} = \mathbf{t} \times \mathbf{n} = \frac{p}{(r_0^2 + p^2)^{\frac{1}{2}}} \left[\sin \left(\frac{s}{(r_0^2 + p^2)^{\frac{1}{2}}} \right), -\cos \left(\frac{s}{(r_0^2 + p^2)^{\frac{1}{2}}} \right), \frac{r_0}{p} \right]. \quad (2.5)$$

This triad will be useful below in decomposing the velocity field into intrinsic components.

The circular helix is determined by the curvature

$$c = \frac{1}{R} = |X''| = \frac{r_0}{r_0^2 + p^2}, \quad c \in (0, \infty), \quad (2.6)$$

and, by the third of the Frenet equations $\mathbf{b}' = -\tau\mathbf{n}$, the torsion

$$\tau = \frac{p}{r_0^2 + p^2}, \quad \tau \in (-\infty, \infty). \quad (2.7)$$

For right-handed helices we assume (without loss of generality) $p > 0$, and so $\tau > 0$. The pitch angle δ (which measures the slope of the helix), is given by

$$\tan \delta = \frac{p}{r_0} = \frac{\tau}{c}. \quad (2.8)$$

Let σ (> 0) denote the radius of the circular cross-section of the vortex filament, ε the thinness parameter and $\hat{\tau}$ the dimensionless torsion defined by

$$\varepsilon = \frac{\sigma}{R} \quad (\varepsilon \ll 1), \quad \text{and} \quad \hat{\tau} = \tau R \quad (\hat{\tau} \in \mathbb{R}_+). \quad (2.9)$$

It is worth mentioning the case of minimum pitch (minimum distance between two consecutive coils of the helix, measured in a direction parallel to the z -axis). Evidently $z_{min} = 2\pi p_{min} = 2\sigma$, or $p_{min} = \sigma/\pi$. From (2.6) we have

$$R \geq r_0 \left(1 + \frac{p_{min}^2}{r_0^2} \right) = r_0 \left[1 + \left(\frac{\sigma}{\pi r_0} \right)^2 \right]. \quad (2.10)$$

Since $R > r_0$ and $\hat{\tau} = p/r_0$, we can also write

$$\hat{\tau} \geq \frac{p_{min}}{r_0} = \frac{\varepsilon R}{\pi r_0} > \frac{\varepsilon}{\pi}. \quad (2.11)$$

A family of helices $\mathcal{H}_c = \mathcal{H}_c(\tau)$ having equal curvature and different torsion may be found by keeping the curvature constant: from (2.6), (2.7) and for $c = 1/R = \text{constant}$, $\mathcal{H}_c(\hat{\tau})$ is parametrized by

$$\hat{p} = \pm [\hat{r}_0(1 - \hat{r}_0)]^{\frac{1}{2}}, \quad \hat{\tau} = \pm \left(\frac{1 - \hat{r}_0}{\hat{r}_0} \right)^{\frac{1}{2}}, \quad (2.12)$$

where $\hat{r}_0 = r_0/R$ and $\hat{p} = p/R$. Note that $\hat{p} = \hat{p}(\hat{\tau})$ is quadratic in the argument and has two zeros as $\hat{\tau} \rightarrow 0$ and $\hat{\tau} \rightarrow \infty$, so that the helix degenerates to a straight line (in a rather peculiar manner) when

$$\left. \begin{array}{l} p \rightarrow 0, \quad r_0 \rightarrow 0, \quad p/r_0 \rightarrow \infty \\ \hat{p} \sim 1/\hat{\tau}, \quad \text{and} \quad \hat{r}_0 \sim 1/\hat{\tau}^2 \end{array} \right\} \text{as } \hat{\tau} \rightarrow \infty.$$

3. The prescription of Moore & Saffman applied to helices of any pitch

We apply the prescription of Moore & Saffman (1972) to study the influence of torsion on the motion of helical vortex filaments of any pitch. With the assumptions made, the induced velocity at $X_0 \in \mathcal{H}$ (from Moore & Saffman 1972, equation 9.5, with $V_E = W = v = 0$, $V_I = U_I$ and $\mu = 1$) is given by

$$\mathbf{v}(X_0) = \frac{\kappa}{4\pi} \int \left[\mathbf{t} \times \frac{(X_0 - X^*)}{|X_0 - X^*|^3} ds - \mathbf{t}_\circ \times \frac{(X_0 - X_\circ)}{|X_0 - X_\circ|^3} ds_\circ \right] + \mathbf{v}_\circ(X_0), \quad (3.1)$$

with $\mathbf{t}_\circ = dX_\circ/ds_\circ$; X_\circ is the osculating circle at $X_0 \in \mathcal{H}$ (where $s \equiv s_\circ = 0$, $\alpha = 0$), and \mathbf{v}_\circ is its velocity (see figure 2).

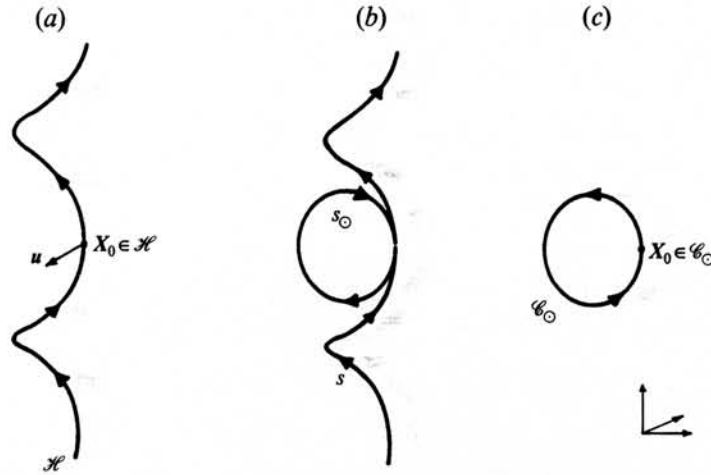


FIGURE 2. Geometric interpretation of the prescription of Moore & Saffman (1972). (a) The velocity field due to a helical vortex filament can be decomposed in two parts, given by (b) subtracting and (c) adding an osculating vortex ring.

The helix \mathcal{H} is given by (2.1), with tangent, normal and binormal given by (2.3)–(2.5); curvature and torsion are given by (2.6) and (2.7). At $\alpha = 0$, $X = X_0 = (r_0, 0, 0)$ and

$$\left. \begin{aligned} t_0 = t(X_0) &= (r_0^2 + p^2)^{-\frac{1}{2}} (0, r_0, p), \\ n_0 = n(X_0) &= (-1, 0, 0), \\ b_0 = b(X_0) &= (r_0^2 + p^2)^{-\frac{1}{2}} (0, -p, r_0). \end{aligned} \right\} \quad (3.2)$$

Let us evaluate the first integrand in (3.1). Since $X^* = (r_0 \cos \alpha, r_0 \sin \alpha, p\alpha)$ and $rd s = dX^*$, we can write

$$dX^* \times (X_0 - X^*) = r_0 p \left\{ \begin{array}{l} -\alpha \cos \alpha + \sin \alpha \\ 1 - \cos \alpha - \alpha \sin \alpha \\ (r_0/p)[\sin^2 \alpha - (1 - \cos \alpha) \cos \alpha] \end{array} \right\} d\alpha. \quad (3.3)$$

We are interested in the contribution to the induced velocity at X_0 along the binormal direction; by (3.2) and (3.3) we have

$$b_0 \cdot [dX^* \times (X_0 - X^*)] = \frac{r_0}{(r_0^2 + p^2)^{\frac{1}{2}}} [p^2 \alpha \sin \alpha + (r_0^2 - p^2)(1 - \cos \alpha)] d\alpha. \quad (3.4)$$

Also

$$|X_0 - X^*|^2 = 2r_0^2(1 - \cos \alpha) + p^2 \alpha^2, \quad (3.5)$$

so that

$$\frac{b_0 \cdot [dX^* \times (X_0 - X^*)]}{|X_0 - X^*|^3} = \frac{r_0}{(r_0^2 + p^2)^{\frac{1}{2}}} \frac{p^2 \alpha \sin \alpha + (r_0^2 - p^2)(1 - \cos \alpha)}{[2r_0^2(1 - \cos \alpha) + p^2 \alpha^2]^{\frac{3}{2}}} d\alpha. \quad (3.6)$$

Note that near $\alpha = 0$, $\sin \alpha \sim \alpha$ and $\cos \alpha \sim 1 - \alpha^2/2$ so that the right-hand side of

(3.6) behaves like

$$\frac{r_0}{(r_0^2 + p^2)^{\frac{1}{2}}} \frac{(r_0^2 + p^2)\alpha^2 d\alpha}{2(r_0^2\alpha^2 + p^2\alpha^2)^{\frac{1}{2}}} = \frac{r_0}{2(r_0^2 + p^2)} \frac{d\alpha}{\alpha}, \quad (3.7)$$

characteristic of the logarithmic singularity at $\alpha = 0$.

Let us now evaluate the second integrand in (3.1). At the point of osculation we identify $s = 0$ ($\alpha = 0$) on the helix with $s_{\circ} = 0$ ($\alpha_{\circ} = 0$) on the osculating circle. By definition of osculation (i.e. the same tangent and the same centre of curvature) we need to have the same Frenet frame $(\mathbf{t}_0, \mathbf{n}_0, \mathbf{b}_0)$ at X_0 and the same intrinsic description. With reference to figure 2(b), $s_{\circ} \equiv s \in [-\pi R, \pi R]$ denotes arclength on the osculating circle X_{\circ} . Moreover, since $s = \alpha (r_0^2 + p^2)^{\frac{1}{2}}$ on the helix and $s_{\circ} = R\alpha_{\circ}$ on the osculating circle, $s_{\circ} \equiv s$ yields

$$\alpha_{\circ} = \alpha [1 + (p/r_0)^2]^{\frac{1}{2}} = \alpha (1 + \hat{t}^2)^{\frac{1}{2}} \quad \text{for } \alpha \in [-\pi, \pi]. \quad (3.8)$$

The osculating circle \mathcal{C}_{\circ} lies in the $(\mathbf{t}_0, \mathbf{n}_0)$ -plane and is centred at

$$X_c = X_0 + \frac{1}{c}\mathbf{n}_0 = (r_0, 0, 0) + \frac{r_0^2 + p^2}{r_0}(-1, 0, 0) = \left(-\frac{p^2}{r_0}, 0, 0\right). \quad (3.9)$$

A point $X_{\circ} \in \mathcal{C}_{\circ}$ is given by

$$\begin{aligned} X_{\circ} &= \left(-\frac{p^2}{r_0}, 0, 0\right) + \frac{1}{c}(\mathbf{t}_0 \sin \alpha_{\circ} - \mathbf{n}_0 \cos \alpha_{\circ}) \\ &= \left(-\frac{p^2}{r_0} + \frac{r_0^2 + p^2}{r_0} \cos \alpha_{\circ}, (r_0^2 + p^2)^{\frac{1}{2}} \sin \alpha_{\circ}, \frac{p}{r_0} (r_0^2 + p^2)^{\frac{1}{2}} \sin \alpha_{\circ}\right), \end{aligned} \quad (3.10)$$

so that

$$\frac{\mathbf{b}_0 \cdot dX_{\circ} \times (X_0 - X_{\circ})}{|X_0 - X_{\circ}|^3} = \frac{r_0 d\alpha_{\circ}}{2^{\frac{1}{2}}(r_0^2 + p^2)(1 - \cos \alpha_{\circ})^{\frac{1}{2}}}. \quad (3.11)$$

Note that near $\alpha_{\circ} = 0$ ($\equiv \alpha = 0$) equation (3.11) behaves like

$$\frac{r_0 d\alpha_{\circ}}{2^{\frac{1}{2}}(r_0^2 + p^2)(1 - \cos \alpha_{\circ})^{\frac{1}{2}}} \sim \frac{r_0}{2(r_0^2 + p^2)} \frac{d\alpha_{\circ}}{\alpha_{\circ}}, \quad (3.12)$$

which coincides with the right-hand side of equation (3.7).

We can now calculate the binormal component of the velocity at $X = X_0$. Taking

$$f(s) = \mathbf{t} \times \frac{(X_0 - X^*)}{|X_0 - X^*|^3}, \quad g(s_{\circ}) = \mathbf{t}_{\circ} \times \frac{(X_0 - X_{\circ})}{|X_0 - X_{\circ}|^3},$$

the integral in (3.1) can be rewritten as

$$\int_{\mathcal{H} - \mathcal{C}_{\circ}} [f(s) ds - g(s_{\circ}) ds_{\circ}] = 2 \left(\int_0^{\pi R} [f(s) - g(s)] ds + \int_{\pi R}^{\infty} f(s) ds \right)$$

since $g(s_{\circ})$ is defined only on the osculating circle (where $s \equiv s_{\circ}$).

In the case of uniform vorticity distribution, the osculating vortex ring propagates with velocity (Fraenkel 1970; Saffman 1970) v_{\circ} , given by

$$v_{\circ}(X_0) = v_{\circ} \mathbf{b}_0 = \frac{\kappa}{4\pi R} \left(\ln \frac{8R}{\sigma} - \frac{1}{4} \right) \mathbf{b}_0. \quad (3.13)$$

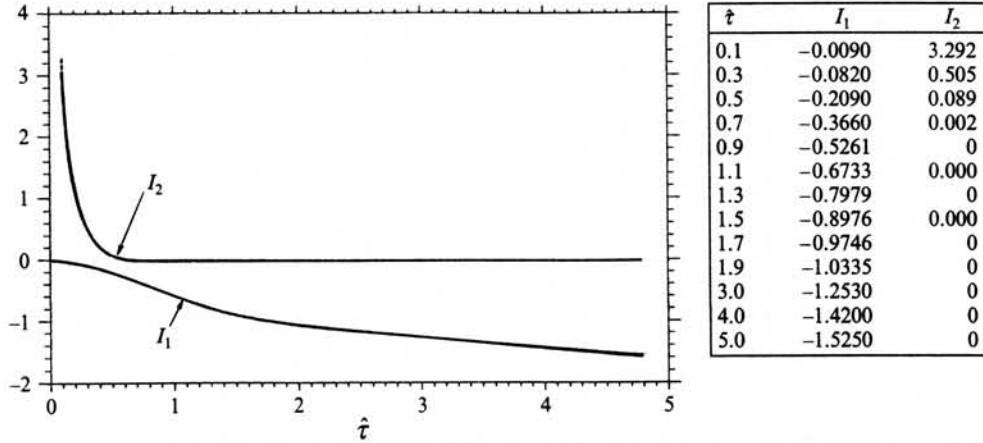


FIGURE 3. I_1 and I_2 , given by equations (3.16) and (3.17), plotted against dimensionless torsion $\hat{\tau}$.

Thus, by (3.6) and (3.11), the binormal component of (3.1) takes the form

$$\hat{v}_b = \hat{v}(X_0) \cdot \mathbf{b}_0 = \ln \frac{1}{\varepsilon} + C_{MS} = 2(I_1 + I_2) + \hat{v}_\odot, \quad (3.14)$$

where

$$C_{MS} = C_{MS}(\hat{\tau}) = 2(I_1 + I_2) + \ln 8 - \frac{1}{4} \quad (3.15)$$

denotes the remainder term obtained by applying the prescription of Moore & Saffman, and where I_1 and I_2 , rewritten in terms of dimensionless torsion, are given by

$$I_1 = \int_0^{\pi(1+\hat{\tau}^2)^{\frac{1}{2}}} \left\{ (1+\hat{\tau}^2)^{\frac{1}{2}} \frac{\hat{\tau}^2 \alpha \sin \alpha + (1-\hat{\tau}^2)(1-\cos \alpha)}{[2(1-\cos \alpha) + (\hat{\tau}\alpha)^2]^{\frac{3}{2}}} - \frac{1}{2^{\frac{1}{2}} \left\{ (1+\hat{\tau}^2) \left[1 - \cos \left(\frac{\alpha}{(1+\hat{\tau}^2)^{\frac{1}{2}}} \right) \right] \right\}^{\frac{1}{2}}} \right\} d\alpha, \quad (3.16)$$

and

$$I_2 = \int_{\pi(1+\hat{\tau}^2)^{\frac{1}{2}}}^{\infty} (1+\hat{\tau}^2)^{\frac{1}{2}} \frac{\hat{\tau}^2 \alpha \sin \alpha + (1-\hat{\tau}^2)(1-\cos \alpha)}{[2(1-\cos \alpha) + (\hat{\tau}\alpha)^2]^{\frac{3}{2}}} d\alpha. \quad (3.17)$$

Note that I_1 is convergent at $\alpha = 0$ and I_2 is convergent at $\alpha = \infty$. The functions $I_1(\hat{\tau})$, $I_2(\hat{\tau})$, obtained by numerical integration, are shown in figure 3.

3.1. Derivation of the Kelvin régime from the Moore & Saffman prescription: helices of large pitch

Kelvin (1880; hereafter denoted by K) considers the case of $\hat{\tau} \gg 1$ (helices of large pitch) and $r_0 \ll \sigma$ (see figure 4), where a helical vortex filament of large wavelength is obtained by a linear perturbation from a columnar vortex. The disturbance is given

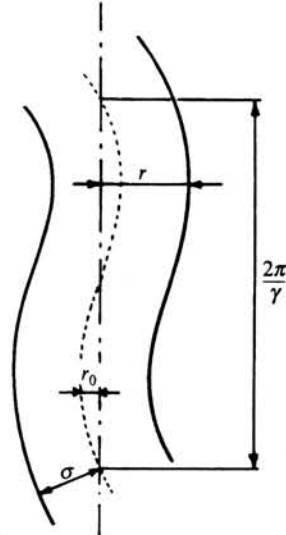


FIGURE 4. Perturbation from a columnar vortex according to Kelvin (1880).

by

$$r = \sigma + r_0 \cos \gamma z \sin (nt - m\theta), \tag{3.18}$$

superimposed on the boundary of the vortex core. In the limit $\hat{t} \rightarrow \infty$, Kelvin considers the case of uniform vorticity distribution (case III in K, where $a = \sigma$, $m = \gamma = p^{-1}$ and $\omega = \kappa/2\pi\sigma^2$) and he finds (p. 167, equation 61) that the angular velocity ($-n$ in K) with which the disturbance travels round the original vortex is given (to leading order) by

$$-n = \frac{\kappa\gamma^2}{4\pi} \left(\ln \frac{1}{\gamma\sigma} + \frac{1}{4} + 0.1159\dots \right) \quad (\hat{t} \gg 1), \tag{3.19}$$

where $0.1159\dots = -\ln 2 - E$ and $E = 0.5772\dots$ is Euler's constant. Since $\hat{t} \sim \hat{p}^{-1} = \gamma R$ as $\hat{t} \rightarrow \infty$, we have

$$\hat{v}_b = \ln \frac{1}{\epsilon} + C_K : \quad C_K = C_K(\hat{t}) = -\ln \hat{t} + \frac{1}{4} + \ln 2 - E \quad (\hat{t} \gg 1), \tag{3.20}$$

where C_K denotes the remainder term obtained by K.

The following result can now be proved.

LEMMA 1. $\lim_{\hat{t} \rightarrow \infty} C_{MS} = C_K$.

Proof. Let us consider the integrands in (3.16) and (3.17). For $\hat{t} \gg 1$ we have

$$F(\alpha) = (1 + \hat{t}^2)^{\frac{1}{2}} \frac{\hat{t}^2 \alpha \sin \alpha + (1 - \hat{t}^2)(1 - \cos \alpha)}{[2(1 - \cos \alpha) + (\hat{t}\alpha)^2]^{\frac{3}{2}}} \sim \frac{\alpha \sin \alpha - (1 - \cos \alpha)}{\alpha^3} = \bar{F}(\alpha), \tag{3.21}$$

and for $0 \leq \alpha \leq \alpha_0$ ($\alpha_0 \ll 1$)

$$G(\alpha) = \frac{1}{2^{\frac{3}{2}} \left\{ (1 + \hat{t}^2) \left[1 - \cos \left(\alpha / (1 + \hat{t}^2)^{\frac{1}{2}} \right) \right] \right\}^{\frac{3}{2}}} \sim \frac{1}{2\alpha} = \bar{G}(\alpha); \tag{3.22}$$

thus we can write

$$I_1 + I_2 \sim \int_0^{\alpha_0} [\bar{F}(\alpha) - \bar{G}(\alpha)] d\alpha + \int_{\alpha_0}^{\pi\hat{\tau}} [\bar{F}(\alpha) - G(\alpha)] d\alpha + \int_{\pi\hat{\tau}}^{\infty} \bar{F}(\alpha) d\alpha. \quad (3.23)$$

Contributions from the first and the third integrals in the right-hand side of (3.23) are certainly negligible: for values near $\alpha = 0$, we have

$$\lim_{\alpha \rightarrow 0} [\bar{F}(\alpha) - \bar{G}(\alpha)] = 0, \quad (3.24)$$

while for $\alpha \geq \pi\hat{\tau}$ ($\hat{\tau} \gg 1$) we can write

$$\int_{\pi\hat{\tau}}^{\infty} \bar{F}(\alpha) d\alpha \sim \int_{\pi\hat{\tau}}^{\infty} \frac{d\alpha}{\alpha^2} \sim \frac{1}{\pi\hat{\tau}}, \quad (3.25)$$

which is negligible for $\hat{\tau} \gg 1$. Hence

$$\begin{aligned} \lim_{\hat{\tau} \rightarrow \infty} (I_1 + I_2) &= \lim_{\substack{\hat{\tau} \rightarrow \infty \\ \alpha_0 \rightarrow 0}} \int_{\alpha_0}^{\pi\hat{\tau}} [\bar{F}(\alpha) - G(\alpha)] d\alpha \\ &= \lim_{\alpha_0 \rightarrow 0} \int_{\alpha_0}^{\infty} \frac{\alpha \sin \alpha - (1 - \cos \alpha)}{\alpha^3} d\alpha - \lim_{\substack{\hat{\tau} \rightarrow \infty \\ \alpha_0 \rightarrow 0}} \int_{\alpha_0}^{\pi\hat{\tau}} \frac{d\alpha}{2^{\frac{1}{2}} \hat{\tau} [1 - \cos(\alpha/\hat{\tau})]^{\frac{1}{2}}}. \end{aligned} \quad (3.26)$$

The first integral in the right-hand side of (3.26) can be expressed by means of integral representations of Euler's constant (Gradshteyn & Ryzhik 1980, 3.783.1 and 8.367.8), i.e.

$$\int_{\alpha_0}^{\infty} \frac{\alpha \sin \alpha - (1 - \cos \alpha)}{\alpha^3} d\alpha = \frac{1}{2} \left[\frac{1}{2} - E - \ln \alpha_0 + O(\alpha_0^2) \right], \quad (3.27)$$

while for the second integral we have

$$\begin{aligned} \int_{\alpha_0}^{\pi\hat{\tau}} \frac{d\alpha}{2^{\frac{1}{2}} \hat{\tau} [1 - \cos(\frac{\alpha}{\hat{\tau}})]^{\frac{1}{2}}} &= \int_{\alpha_0/\hat{\tau}}^{\pi} \frac{d\varphi}{2^{\frac{1}{2}} (1 - \cos \varphi)^{\frac{1}{2}}} \\ &= \frac{1}{2} \int_{\alpha_0/2\hat{\tau}}^{\pi/2} \frac{d\psi}{\sin \psi} = \frac{1}{2} \left\{ \ln \hat{\tau} + 2 \ln 2 - \ln \alpha_0 + O \left[\left(\frac{\alpha_0}{\hat{\tau}} \right)^2 \right] \right\}. \end{aligned} \quad (3.28)$$

Thus, by (3.15), we have

$$\lim_{\hat{\tau} \rightarrow \infty} C_{MS} = \lim_{\hat{\tau} \rightarrow \infty} \left[2(I_1 + I_2) + \ln 8 - \frac{1}{4} \right] = \lim_{\hat{\tau} \rightarrow \infty} \left(-\ln \hat{\tau} + \frac{1}{4} + \ln 2 - E \right) = C_K \quad (3.29)$$

which proves the statement. \square

4. Comparative analysis and numerical results

4.1. Analysis based on the re-elaboration of Hardin's approach

Hardin's (1982) approach is based on a particular transform of the Biot-Savart integral (decomposed in Cartesian components) and the derivation of the velocity field in cylindrical polar components u_r, u_α, u_z in the region interior ($r < r_0$) and exterior ($r > r_0$) to the cylinder on which the helix is inscribed (see equations 8 and 9 of Hardin's paper). In order to determine the induced velocity at points asymptotically near the vortex filament centreline, we consider the points which lie on the helical surface given by $\alpha_0 = \alpha^* - z/p = 0$ (α^* denotes the polar coordinate; $\alpha_0 \equiv \psi$ and $\alpha^* \equiv \phi$ in Hardin's notation). By (2.3)–(2.5), the velocity field $\mathbf{u} = u_\alpha(-\mathbf{i} \sin \alpha + \mathbf{j} \cos \alpha) + u_z \mathbf{k}$ can be rewritten in intrinsic components (u_t, u_n, u_b), that is

$$u_t = \frac{r_0 u_\alpha + p u_z}{(r_0^2 + p^2)^{\frac{1}{2}}}, \quad u_n = 0, \quad u_b = -\frac{p u_\alpha - r_0 u_z}{(r_0^2 + p^2)^{\frac{1}{2}}}. \quad (4.1)$$

The relative displacement in the fluid is given only by u_b , while u_t yields pure tangential motion along the helix. Thus, by equation (8) of Hardin, the binormal component of the velocity for the interior region is given by

$$u_b|_{r < r_0} = \frac{\kappa}{\pi (r_0^2 + p^2)^{\frac{1}{2}}} \left[\frac{r_0}{2p} - \left(\frac{r_0}{r} + \frac{r_0^2}{p^2} \right) \mathcal{Q}(r, 0) \right], \quad (4.2)$$

while, using equation (9) of Hardin, for the exterior region we have

$$u_b|_{r > r_0} = \frac{-\kappa}{\pi (r_0^2 + p^2)^{\frac{1}{2}}} \left[\frac{1}{2} \frac{p}{r} + \left(\frac{r_0}{r} + \frac{r_0^2}{p^2} \right) \mathcal{P}(r, 0) \right]. \quad (4.3)$$

$\mathcal{P}(r, 0)$ and $\mathcal{Q}(r, 0)$ are series expressed in terms of (modified) Bessel functions of integer order and, in general, are functions of r_0, p, r, α_0 (cf. Hardin's expressions).

Two limit cases present themselves when $r_0 \rightarrow 0$ and when $p \rightarrow 0$ (in reality r_0 and p are bounded from below respectively by $r_{0, \min} = \sigma (> 0)$ and $p_{\min} = \sigma/\pi$).

(i) *Rectilinear vortex filament.* Let us consider the case $r_0 \rightarrow 0$, for p fixed. In this case the helix approaches its central axis; ideally, if we let $\sigma \rightarrow 0$, then the rectilinear vortex filament solution is recovered. From (2.5) and (2.6), this yields $\lim_{r_0 \rightarrow 0} c = 0$, and $\lim_{r_0 \rightarrow 0} \mathbf{b} = [\sin(s/p), -\cos(s/p), 0]$ and from equations (4.1), as $r_0 \rightarrow 0$, $u_r = u_z = 0$ and $u_\alpha = \kappa/2\pi r$; thus, denoting by \mathbf{q} the rotational unit vector, we have $\lim_{r_0 \rightarrow 0} \mathbf{u} = [\kappa/(2\pi r)]\mathbf{q}$, with the streamlines concentric circles about the central axis (see figure 5a).

(ii) *Cylindrical vortex sheet.* Consider now the case $p \rightarrow 0$, for r_0 fixed. In this case the coils of the helix are flattened down and packed together. As an ideal case, let $\sigma \rightarrow 0$: the cylinder in which the helix is inscribed becomes an infinite cylindrical vortex sheet and a circular cylindrical jet is realized (figure 5b). The velocity field is discontinuous across the vortex sheet: as $p \rightarrow 0$, the arguments of the modified Bessel functions in the series of (4.2) (see the expression for $\mathcal{Q}(r, 0) \equiv S_1(\rho, 0)$ in equation 8 of Hardin's paper) tend to infinity, and the product of the series can be calculated by asymptotic expansions for large arguments (Abramowitz & Stegun 1965). To leading order and for $r_0 > r$, we have

$$\lim_{p \rightarrow 0} \mathcal{Q}(r, 0) = \lim_{p \rightarrow 0} \left[-\frac{p}{2\nu (r_0 r)^{\frac{1}{2}}} \sum_{v=1}^{\infty} e^{-\nu \frac{(r_0 - r)}{p}} (1 + \dots) \right] = 0. \quad (4.4)$$

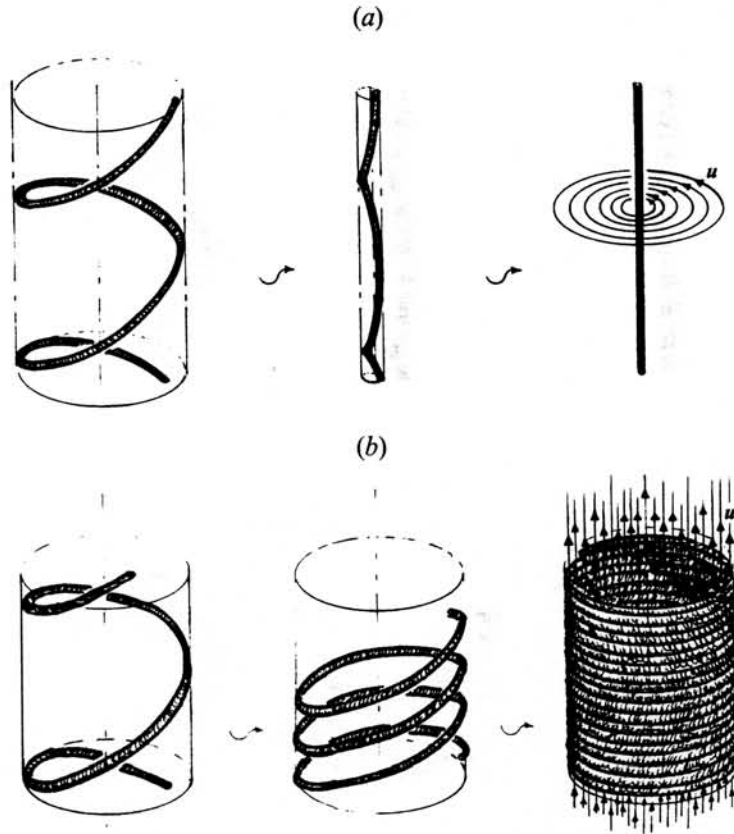


FIGURE 5. (a) As $r_0 \rightarrow 0$, keeping p fixed, the helical vortex filament approaches the z -axis and forms a rectilinear vortex filament. (b) As $p \rightarrow 0$, keeping r_0 fixed, the coils of the helix are flattened down and form a cylindrical vortex sheet.

Combining this result with (4.2) and taking the limit, we have

$$\lim_{p \rightarrow 0} u_b|_{r < r_0} = \lim_{p \rightarrow 0} \frac{\kappa}{2\pi p} = +\infty. \quad (4.5)$$

Similarly, we can evaluate the limit for the exterior region. We have

$$\lim_{p \rightarrow 0} u_b|_{r > r_0} = -\frac{\kappa}{\pi r} \lim_{p \rightarrow 0} \left(1 + \frac{rr_0}{p^2}\right) \mathcal{P}(r, 0) = 0, \quad (4.6)$$

so that asymptotically we have $[u_b] = (\kappa/2\pi p)$ across the cylindrical vortex sheet.

4.1.1. Remainder term of the binormal component of the velocity and numerical results

The binormal component of the velocity can be evaluated asymptotically at two points P and Q lying on the exterior and interior boundary of the vortex core along the normal direction. In polar coordinates (r, θ) centred on the vortex core, the two points are given by: $P = (r_0 + \sigma, \pi)$ and $Q = (r_0 - \sigma, 0)$. The remainder term C is determined by comparing equation (1.2) (using 1.3) with (4.2) and (4.3). Since $\hat{u}^{(a)} \cdot \mathbf{b} = \hat{u}_b$ (where overhats denote quantities in dimensionless form), we have

$$\frac{2}{\varepsilon} \mathbf{q} \cdot \mathbf{b} + \ln \frac{1}{\varepsilon} + C = \frac{1}{(r_0^2 + p^2)^{\frac{1}{2}}} (p \hat{u}_x - r_0 \hat{u}_z). \quad (4.7)$$

At Q we have $r = r_0 - \varepsilon R$ and $\hat{v}_b^{(a)} = \hat{u}_b^{(a)} - 2/\varepsilon$. Let us consider the family of helices $\mathcal{H}_c = \mathcal{H}_c(\hat{\tau})$. After some algebraic manipulation, (4.2) can be rewritten in dimensionless form as follows:

$$\hat{v}|_{int} = 2 \frac{(1 + \hat{\tau}^2)^{\frac{1}{2}}}{\hat{\tau}} - \frac{4(1 - \varepsilon)(1 + \hat{\tau}^2)^{\frac{3}{2}}}{\hat{\tau}^2[1 - \varepsilon(1 + \hat{\tau}^2)]} \mathcal{Q}(\varepsilon, \hat{\tau}) - \frac{2}{\varepsilon}, \tag{4.8}$$

where

$$\mathcal{Q}(\varepsilon, \hat{\tau}) = \sum_{v=1}^{\infty} v K'_v(vz_K) I_v(vz_I), \quad z_K = \frac{1}{\hat{\tau}}, \quad z_I = \frac{1 - \varepsilon(1 + \hat{\tau}^2)}{\hat{\tau}}. \tag{4.9}$$

Similarly for the velocity field at P , where $r = r_0 + \varepsilon R$ and $\hat{v}_b^{(a)} = \hat{u}_b^{(a)} + 2/\varepsilon$. After some algebra, we have

$$\hat{v}|_{ext} = -\frac{2\hat{\tau}(1 + \hat{\tau}^2)^{\frac{1}{2}}}{1 + \varepsilon(1 + \hat{\tau}^2)} - \frac{4(1 + \varepsilon)(1 + \hat{\tau}^2)^{\frac{3}{2}}}{\hat{\tau}^2[1 + \varepsilon(1 + \hat{\tau}^2)]} \mathcal{P}(\varepsilon, \hat{\tau}) + \frac{2}{\varepsilon}, \tag{4.10}$$

where

$$\mathcal{P}(\varepsilon, \hat{\tau}) = \sum_{v=1}^{\infty} v K_v(vz_K) I'_v(vz_I), \quad z_K = \frac{1 + \varepsilon(1 + \hat{\tau}^2)}{\hat{\tau}}, \quad z_I = \frac{1}{\hat{\tau}}. \tag{4.11}$$

By (4.7), and using (4.8) and (4.10), we have

$$C_H(\varepsilon) = \frac{C_{int} + C_{ext}}{2}, \quad \begin{cases} C_{int} = \hat{v}|_{int} - \ln 1/\varepsilon \\ C_{ext} = \hat{v}|_{ext} - \ln 1/\varepsilon, \end{cases} \tag{4.12}$$

where $C_H(\varepsilon)$ denotes the remainder term obtained by the present re-elaboration of Hardin's approach.

Numerical evaluation of C_{int} and C_{ext} has been carried out (Ricca 1992, 1993) with a high degree of accuracy. Figure 6 illustrates the behaviour of the remainder term C versus the dimensionless torsion $\hat{\tau}$ in the exterior and interior case (that is at P and Q) for ε equal to 0.1, 0.01, 0.001. Numerical instabilities due to the particular coupling of ε and $\hat{\tau}$ have been noticed outside a certain range of $\hat{\tau}$ and have limited considerably the investigation.

In any case the dependence of C on $\hat{\tau}$ is clear and significant. In figure 6(a) ($\varepsilon = 0.1$) curvature and torsion are of the same order of magnitude and both influence C (although the leading-order effect on the displacement of the vortex filament is due to the local curvature). Note that the 'interior' and the 'exterior' curves are separated by a distance of the order of the diameter of the vortex cross-section, which is visibly decreasing as $\hat{\tau}$ increases; at about $\hat{\tau} = 1$, this is nearly equal to the dimensionless diameter of the vortex. The superposition of induced effects seems sensitive to the fact that the smaller $\hat{\tau}$ is, the greater is the difference between the values of the corresponding streamlines in the interior and the exterior region. For smaller ε the distance between the two curves tends to become smaller (figure 6b, c). Numerical instabilities become more relevant in figure 6(c), as we move away from the central region of the diagram.

4.2. Re-elaboration of the results obtained by Levy & Forsdyke and Widnall for helices of small pitch

The results obtained by Levy & Forsdyke (1928; hereafter denoted by LF) and by Widnall (1972; hereafter denoted by W) for helices of moderate pitch (and by using

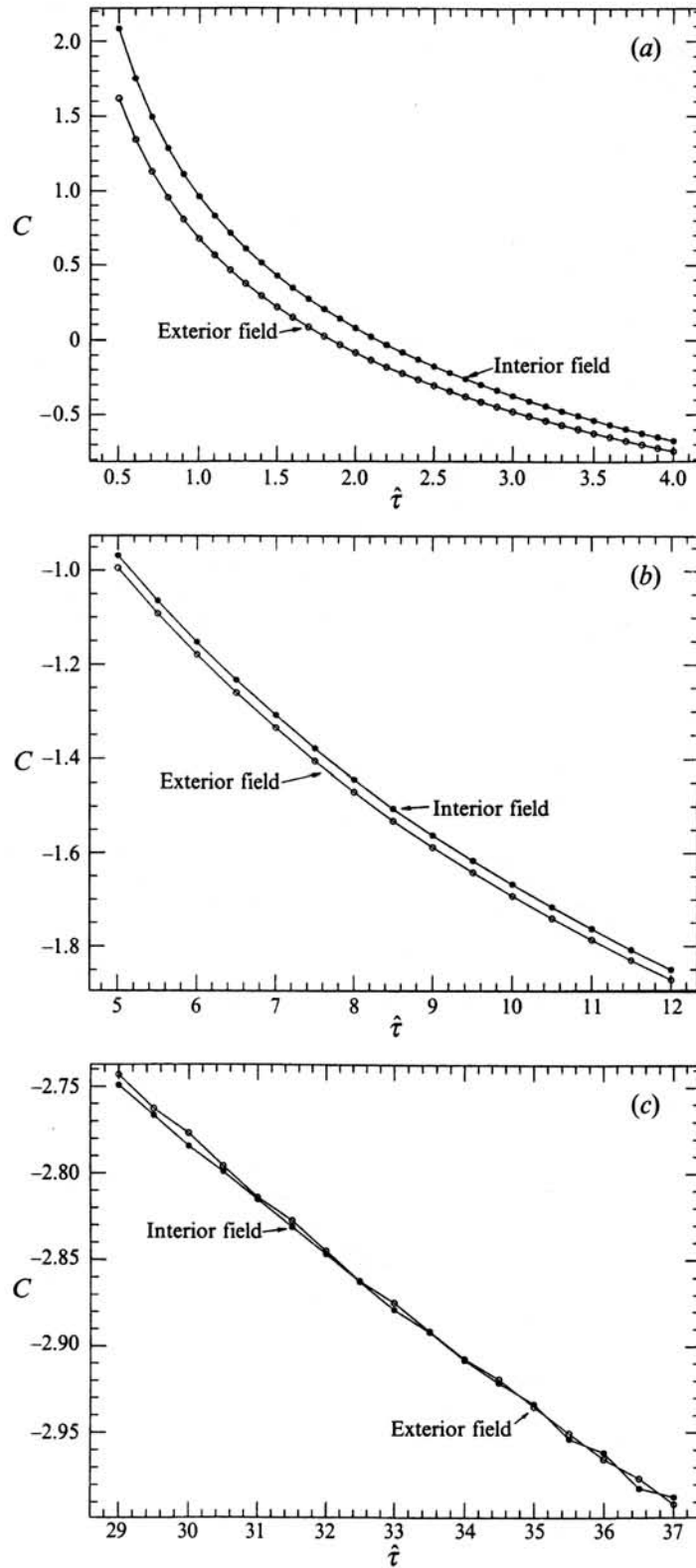


FIGURE 6. Remainder term C plotted against dimensionless torsion $\hat{\tau}$. Interior and exterior field at boundary points for (a) $\epsilon = 0.1$; (b) $\epsilon = 0.01$; (c) $\epsilon = 0.001$.

different methods), can be re-elaborated for comparison. The results presented in LF and in W are given in terms of translational velocity (V) and rotational velocity (Ω) of the helix (with respect to a reference fixed with the z -axis).

The binormal component of the velocity field expressed as a function of V and Ω is given by

$$v_b = \ln \frac{1}{\varepsilon} + C = \frac{r_0}{(r_0^2 + p^2)^{\frac{1}{2}}} (V - p\Omega) \quad (4.13)$$

(note that the rotational component about the vortex filament centreline does not contribute to the displacement of the vortex filament in the fluid); by different numerical methods, LF and W obtained V and Ω as functions of the tangent to the pitch angle. In particular, LF make the assumption $(\sigma/r_0) = 0.1$, which implies $\varepsilon = [10(1 + \hat{\tau}^2)]^{-1}$ (LF consider $0.25 \leq \hat{\tau} \leq 1.25$, hence $0.04 \leq \varepsilon \leq 0.08$). In our notation, we have

$$\hat{V}_{LF} = \frac{V}{\kappa/2\pi r_0} = \frac{1}{2} \frac{r_0}{R} \left(\frac{V}{\kappa/4\pi R} \right) = \frac{1}{2(1 + \hat{\tau}^2)} \hat{V}, \quad (4.14)$$

and

$$\hat{\Omega}_{LF} = \frac{\Omega}{\kappa/2\pi r_0^2} = \frac{1}{2} \left(\frac{r_0}{R} \right)^2 \left(\frac{\Omega}{\kappa/4\pi R^2} \right) = \frac{1}{2(1 + \hat{\tau}^2)^2} \hat{\Omega}, \quad (4.15)$$

where \hat{V} and $\hat{\Omega}$ are the dimensionless velocities read directly from the diagram presented in LF (p. 689, figure 2). By the relations above, we have

$$\bar{C}_{LF} = \bar{C}_{LF}(\hat{\tau}) = 2(1 + \hat{\tau}^2)^{\frac{1}{2}} (\hat{V}_{LF} - \hat{\tau} \hat{\Omega}_{LF}) - \ln(1 + \hat{\tau}^2) - \ln 10, \quad (4.16)$$

where \bar{C}_{LF} denotes the remainder term obtained by LF (the overbar indicates that the assumption $\varepsilon = [10(1 + \hat{\tau}^2)]^{-1}$ has been made).

Widnall uses the 'cut-off' approximation and numerical integration. The translational velocity V (W, equation 54) in our notation is given by

$$V = \frac{\kappa}{4\pi r_0} \left[-V_{A1} \left(\ln \frac{\sigma}{r_0} - A \right) + V_{A1} \right], \quad (4.17)$$

and the rotational velocity Ω (W, equation 55) by

$$\Omega = \frac{\kappa}{4\pi r_0^2} \left[-\Omega_1 \left(\ln \frac{\sigma}{r_0} - A \right) + \Omega_1 \right], \quad (4.18)$$

where

$$V_{A1} = V_{A1}(\hat{\tau}) = \frac{1}{\hat{\tau}g(\hat{\tau})}, \quad \Omega_1 = \Omega_1(\hat{\tau}) = -\frac{1}{g(\hat{\tau})}, \quad g(\hat{\tau}) = \frac{\hat{\tau}}{(1 + \hat{\tau}^2)^{\frac{1}{2}}}, \quad (4.19)$$

and $A = \frac{1}{4}$ (uniform vorticity). V_{A1} and Ω_1 are read directly from the diagram shown in W (p. 656, figure 3).

Substituting (4.17) and (4.18) into (4.13) and putting everything in dimensionless form, we have

$$C_W = C_W(\hat{\tau}) = \hat{v} - \ln \frac{1}{\varepsilon} = (1 + \hat{\tau}^2)^{\frac{1}{2}} (V_{A1} - \hat{\tau} \Omega_1) - \ln(1 + \hat{\tau}^2) + \frac{1}{4}, \quad (4.20)$$

where C_W denotes the remainder term obtained by W.

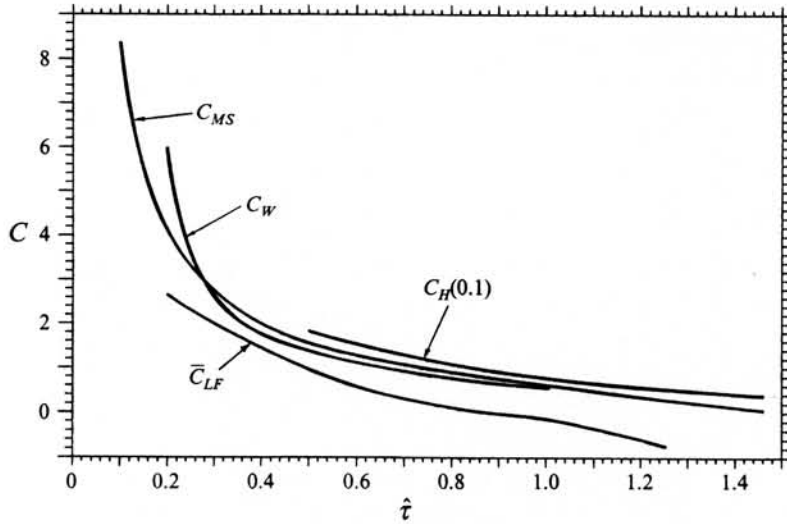


FIGURE 7. Comparative behaviour of $C_H(0.1)$, C_{MS} , C_W and \bar{C}_{LF} plotted against dimensionless torsion $\hat{\tau}$.

4.3. Comparison of results

A full comparison of the results is now possible. In figure 7, $C_H(0.1)$, C_{MS} , C_W and \bar{C}_{LF} are plotted against $\hat{\tau}$ for $0.1 \leq \hat{\tau} \leq 1.5$.

The dependence of the remainder term on $\hat{\tau}$ is evident. Keeping curvature fixed, this means that the binormal component of the induced velocity decreases as torsion increases. For $\hat{\tau} < 0.3$ the difference between C_W and C_{MS} seems to increase notably; this discrepancy is not justified and must be probably due to errors that are associated with direct reading of data from diagrams or present in Widnall's numerical calculations (full agreement between the cut-off approximation and the osculating circle technique can be found also for small $\hat{\tau}$ using equation 8, p. 214 of Saffman 1992). C_{MS} and $C_H(0.1)$ behave very similarly for the full range of $\hat{\tau}$ and remain closely parallel to each other. The small difference between the two curves remains almost constant (and approximately equal to 0.25) as $\hat{\tau}$ increases (note that $C_H(\varepsilon)$, $\varepsilon \neq 0$, is not the limit curve). The curve \bar{C}_{LF} must be considered as a case on its own because of the assumption $\varepsilon = [10(1 + \hat{\tau}^2)]^{-1}$, and because of the limited accuracy of the original calculation (done by a planimeter).

In figure 8, $C_H(\varepsilon)$ ($\varepsilon = 0.1, 0.01, 0.001$), C_{MS} , C_K are plotted against $\hat{\tau}$, for a wider range of $\hat{\tau}$. Again $C_H(\varepsilon)$ ($\varepsilon = 0.1, 0.01, 0.001$) can be regarded as an estimate of the limit curve C_H at $\varepsilon = 0$. As expected, the Kelvin régime ($\hat{\tau} \gg 1$) is recovered in full by C_{MS} .

5. Conclusions

In this paper we have analysed in detail, and for the first time, the rôle of torsion in the dynamics of twisted vortex filaments. We have demonstrated that torsion may influence considerably the motion of helical vortex filaments in an incompressible perfect fluid. The binormal component of the induced velocity, asymptotically responsible for the displacement of the vortex filament in the fluid, has been closely analysed. The study has been performed by applying the prescription of Moore &

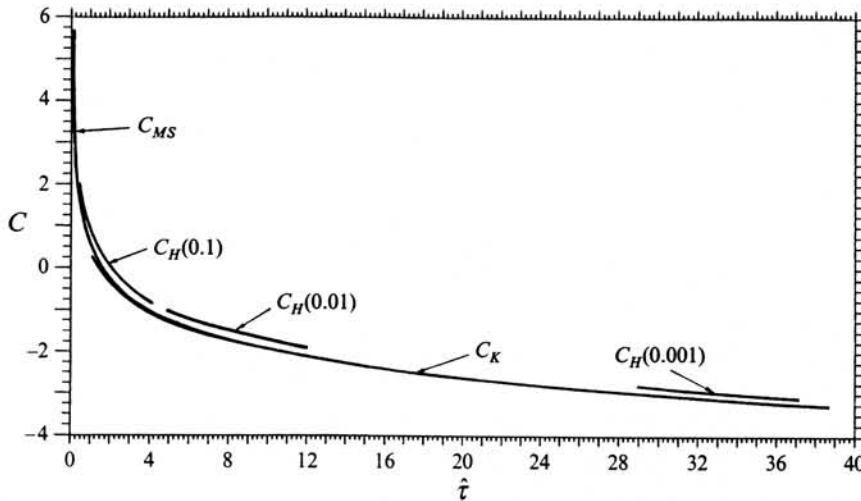


FIGURE 8. Comparative behaviour of $C_H(\varepsilon)$ ($\varepsilon = 0.1, 0.01, 0.001$), C_{MS} , C_K plotted against dimensionless torsion $\hat{\tau}$.

Saffman (1972) to helices of any pitch and a new asymptotic integral formula has been derived. We have also proved that the Kelvin régime and its limit behaviour is obtained as a limit form of that integral asymptotic formula. The results have been compared with new calculations based on the re-elaboration of Hardin's approach (1982) and with results obtained by Levy & Forsdyke (1928) and Widnall (1972) for helices of small pitch, re-elaborated for the purpose. The agreement between different treatments is satisfactory and reassuring.

Although the influence of torsion may be regarded as a higher-order effect in determining the motion of twisted vortex filaments, nevertheless these results show that torsion can be as important as the distribution of vorticity over the cross-section of a vortex filament. The importance of this result is underlined by the fact that the presence of torsion is inherently associated with the three-dimensional character of vortex evolution and the high twisting of vorticity lines. Experimental measurements of \hat{v}_b made by Hopfinger *et al.* (1982) and Leibovich & Ma (1983) that suggested that torsion effects had to be considered as $O(1)$ contributions to the dynamics of vortex filaments have been fully confirmed by our analysis.

I would like to express my deepest gratitude to Professor H.K. Moffatt, for his guidance and continuous support. It was he in particular who helped me to understand and apply the prescription of Moore & Saffman. It is a pleasure to acknowledge the stimulus of several discussions with Professor P.G. Saffman. For advice on computational problems I am indebted to Dr M. Spivack. Most of this research was conducted at DAMTP (Cambridge, UK) and was possible through the Research Fellowship program funded by the Associazione Sviluppo Scientifico e Tecnologico del Piemonte (Turin, Italy). The hospitality of the Institute of Theoretical Physics (Santa Barbara, UCSB) and of the Institute for Advanced Study (Princeton) is acknowledged. Financial support from Trinity College (Cambridge) and from the UK Science and Engineering Research Council Grant GR/G46745 is also acknowledged.

REFERENCES

- ABRAMOWITZ, M. & STEGUN, I. A. 1965 *Handbook of Mathematical Functions*. Dover.
- ADEBIYI, A. 1981 On the existence of steady helical vortex tubes of small cross-section. *Q. J. Mech. Appl. Maths* **34**, 153–177.
- BATCHELOR, G. K. 1967 *An Introduction to Fluid Dynamics*. Cambridge University Press.
- BORATAV, O. N., PELZ, R. B. & ZABUSKY, N. J. 1992 Reconnection in orthogonally interacting vortex tubes: Direct numerical simulations and quantifications. *Phys. Fluids A* **4**, 581–605.
- CALLEGARI, A. J. & TING, L. 1978 Motion of a curved vortex filament with decaying vortical core and axial velocity. *SIAM J. Appl. Maths* **35**, 148–175.
- CROW, S. C. 1970 Stability theory of a pair of trailing vortices. *AIAA J.* **8**, 2172–2179.
- FRAENKEL, L. E. 1970 On steady vortex rings of small cross-section in an ideal fluid. *Proc. R. Soc. Lond. A* **316**, 29–62.
- FUKUMOTO, Y. & MIYAZAKI, T. 1991 Three-dimensional distortions of a vortex filament with axial velocity. *J. Fluid Mech.* **222**, 369–416.
- GRADSHTEYN, I. S. & RYZHIK, I. M. 1980 *Table of Integrals, Series, and Products*. Academic Press.
- HARDIN, J. C. 1982 The velocity field induced by a helical vortex filament. *Phys. Fluids* **25**, 1949–1952.
- HOPFINGER, E. J., BROWAND, F. K. & GAGNE, Y. 1982 Turbulence and waves in a rotating tank. *J. Fluid Mech.* **125**, 505–534.
- KELVIN, LORD 1880 Vibrations of a columnar vortex. *Phil. Mag.* **10**, 155–168.
- KERR, R. M. 1985 Higher-order derivative correlation and the alignment of small-scale structures in isotropic turbulence. *J. Fluid Mech.* **153**, 31–58.
- KIDA, S. 1993 *Tube-Like Structures in Turbulence*. Lecture Notes in Numerical Applied Analysis. Springer (in press).
- KLEIN, R. & MAJDA, A. J. 1991 Self-stretching of a perturbed vortex filament. I. The asymptotic equation for deviations from a straight line. *Physica D* **49**, 323–352.
- LEIBOVICH, S. & MA, H. Y. 1983 Soliton propagation on vortex cores and the Hasimoto soliton. *Phys. Fluids* **26**, 3173–3179.
- LESIEUR, M. (ED.) 1991 *Computational Fluid Dynamics*. Institute de Mécanique de Grenoble, CNRS.
- LEVI-CIVITA, T. 1932 Attrazione Newtoniana dei tubi sottili e vortici filiformi. (Newtonian attraction of slender tubes and filiform vortices.) *Ann. R. Scuola Normale Sup. Pisa* **1**, 1–54.
- LEVY, H. & FORSDYKE, A. G. 1928 The steady motion and stability of a helical vortex. *Proc. R. Soc. Lond. A* **120**, 670–690.
- LUNDGREN, T. S. & ASHURST, W. T. 1989 Area-varying waves on curved vortex tubes with application to vortex breakdown. *J. Fluid Mech.* **200**, 283–307.
- MARSHALL, J. S. 1991 A general theory of curved vortices with circular cross-section and variable core area. *J. Fluid Mech.* **229**, 311–338.
- MAXWORTHY, T., HOPFINGER, E. J. & REDEKOPP, L. G. 1985 Wave motion on vortex cores. *J. Fluid Mech.* **151**, 141–165.
- MOORE D. W. & SAFFMAN P. G. 1972 The motion of a vortex filament with axial flow. *Phil. Trans. R. Soc. Lond. A* **272**, 403–429.
- RICCA, R. L. 1992 Local dynamics of a twisted vortex filament. In *XVIII Intl Congr. Theor. Appl. Mech. - Abstracts*, p. 123. IUTAM.
- RICCA, R. L. 1993 The effect of torsion on the local dynamics of a vortex filament. In *Euromech 305 - Dynamics and Geometry of Vortical Structures*, pp. 39–40. Università di Roma "La Sapienza".
- SAFFMAN, P. G. 1970 The velocity of viscous vortex rings. *Stud. Appl. Maths* **49**, 371–380.
- SAFFMAN, P. G. 1992 *Vortex Dynamics*. Cambridge University Press.
- SHE, Z.-S., JACKSON, E. & ORSZAG, S. A. 1990 Intermittent vortex structures in homogeneous isotropic turbulence. *Nature* **344**, 226–228.
- SIGGIA, E. D. 1981 Numerical study of small scale intermittency in three-dimensional turbulence. *J. Fluid Mech.* **107**, 375–406.
- VINCENT, A. & MENEGUZZI, M. 1991 The spatial structure and statistical properties of homogeneous turbulence. *J. Fluid Mech.* **225**, 1–25.
- WIDNALL, S. E. 1972 The stability of a helical vortex filament. *J. Fluid Mech.* **54**, 641–663.

- WIDNALL, S. E. & BLISS, D. B. 1971 Slender-body analysis of the motion and stability of a vortex filament containing an axial flow. *J. Fluid Mech.* **50**, 335–353.
- WIDNALL, S. E., BLISS, D. B. & ZALAY, A. 1971 Theoretical and experimental study of the stability of a vortex pair. In *Aircraft Wake Turbulence and Its Detection* (ed. J. Olsen *et al.*), pp. 305–338. Plenum.
- WILLMORE, T. J. 1959 *An Introduction to Differential Geometry*. Oxford University Press.